Published in final edited form as:
J Immunol. 2008 August 1; 181(3): 2084–2091.

Drak2 Contributes to West Nile Virus Entry into The Brain and Lethal Encephalitis

Shuhui Wang[*,2], **Thomas Welte**[*,2], **Maureen McGargill**[Π], **Terrence Town**[†,3], **Jesse Thompson**[*], **John F Anderson**[#], **Richard A Flavell**[‡,†], **Erol Fikrig**[§,‡], **Stephen M. Hedrick**[Π], and **Tian Wang**[*,4]

* *Department of Microbiology, Immunology and Pathology, College of Veterinary Medicine & Biomedical Sciences, Colorado State University, Fort Collins, CO 80523*

Π *Department of Biology and Cancer Center, University of California-San Diego, La Jolla, CA 92093*

† *Section of Immunobiology, Yale University School of Medicine, 300 Cedar Street, New Haven, CT 06520*

 # Department of Entomology, Connecticut Agricultural Experiment Station, P. O. Box 1106, New Haven, CT 06504

‡ *The Howard Hughes Medical Institute, Yale University School of Medicine, 300 Cedar Street, New Haven, CT 06520*

§ *Section of Infectious Diseases, Department of Internal Medicine, Yale University School of Medicine, 300 Cedar Street, New Haven, CT 06520*

Abstract

Drak2, a member of the death-associated protein family of serine/threonine kinases, is specifically expressed in T and B cells. In the absence of Drak2, mice are resistant to experimental autoimmune encephalomyelitis due to a decrease in the number of cells infiltrating the central nervous system (CNS). In the present study, we investigated the role of Drak2 in West Nile virus (WNV)-induced encephalitis and found that *Drak2*$^{-/-}$ mice were also more resistant to lethal WNV infection than wild-type mice. Although, *Drak2*$^{-/-}$ mice had an increase in the number of IFN-γ-producing T cells in the spleen after infection, viral levels in the peripheral tissues were not significantly different between these two groups of mice. In contrast, there was a reduced viral load in the brains of *Drak2*$^{-/-}$ mice, which was accompanied by a decrease in the number of *Drak2*$^{-/-}$ CD4^{+} and CD8^{+} T cells in the brain following WNV infection. Moreover, we detected viral antigens in T cells isolated from the spleen or brain of WNV infected mice. These results suggest that following a systemic infection, WNV might cross the blood brain barrier and enter the CNS by being carried by infected infiltrating T cells.

[4] Corresponding Author: Tian Wang, Ph.D., Department of Microbiology, Immunology and Pathology, College of Veterinary Medicine & Biomedical Sciences, Colorado State University, Campus Delivery 1690, Fort Collins, CO 80523. Telephone: (970) 491-2202; Fax: (970) 491-8707; E-mail: tian.wang@colostate.edu.
[2] These authors contributed equally to this work.
[3] Present address: Departments of Biomedical Sciences and Neurosurgery, Maxine Dunitz Neurosurgical Institute, Cedars-Sinai Medical Center, 8700 Beverly Blvd., Los Angeles, CA 90048.

[5] Abbreviations used in this paper: WNV, West Nile virus; Q-PCR, quantitative PCR; IFN, interferon; i.p., intraperitoneally; LD, lethal dose.

Introduction

West Nile virus (WNV), a vector-borne neurotropic flavivirus, has caused annual outbreaks of viral encephalitis in North America since its arrival here in 1999 (1,2). Following initial virus replication at a site peripheral to the central nervous system (CNS), WNV can enter the brain either via a hematogenous pathway or by retrograde axonal transport from a peripheral site (3–5). Severe neurological disease (including encephalitis) and death have been observed in more than 30% of the confirmed WNV cases with a higher frequency in the elderly and immunocompromised (1,2). Currently, no vaccines are available for humans, and treatment is mostly nonspecific and supportive.

The murine model is an effective *in vivo* experimental model to investigate WNV pathogenesis and host immune response to human infections (6–8). Work from animal models has demonstrated that type 1 interferons (IFNs), γδ T cells and humoral immunity are critical in controlling dissemination of WNV (9–15). In addition, $CD4^+$ (16) and $CD8^+$ αβ T-cells (17, 18) contribute to host survival following WNV infection. WNV can gain access to the CNS after a brief viremia in the periphery, a process called neuroinvasion, that may turn a mild viral infection into severe lethal encephalitis (6,19,20). Recent studies have shown that a WNV replication induces a proinflammatory response that modulates the blood brain barrier (BBB) permeability, which in turn may enable viral entry into the brain and induce lethal encephalitis (5,21). Nevertheless, the underlying mechanism(s) in which WNV crosses the BBB and enters the CNS are not yet clearly understood. Once inside the brain, WNV-induced CNS disease might be caused by neuronal degeneration, a direct result of viral infection, and/or by bystander damage from the immune response to the pathogen, including lymphocyte and microglial cell responses (18,22–24). The contributions of direct cell damage by WNV and damage induced by the host immune response in the development of disease are still under investigation.

DAP kinase-related apoptosis inducing kinase-2 (Drak2), is specifically expressed in T and B cells (25,26). Drak2 functions to negatively regulate signals involved in T cell activation (27). T cells from *Drak2*$^{-/-}$ mice exhibited enhanced sensitivity to T cell receptor-mediated stimulation with a reduced requirement for co-stimulation (26). However, *Drak2*$^{-/-}$ mice were shown to be remarkably resistant to experimental autoimmune encephalomyelitis (EAE), and this resistance was due in part, to a reduction of infiltrating cells into the CNS (26). In the present study, we investigated the role of Drak2 in WNV induced encephalitis.

Materials and Methods

Mice

Drak2$^{-/-}$ mice were bred on the C57BL/6 (B6) background and had been fully backcrossed (26). Littermates were used as controls. Experiments were performed with 6- to 14-wk-old animals. Groups were age- and sex-matched for each experiment and were housed under identical conditions. All animal experiments were approved by the Animal Care and Use Committee at Colorado State University.

Infection in mice

We inoculated mice intraperitoneally (i.p.) with 800 plaque-forming units (PFU) (a dose close to LD_{100}) of WNV isolate 2741 in 200 μl of phosphate-buffered saline (PBS) with 5% gelatin. For intracranial (i.c.) infection, we anesthetized mice and infected them with 160 PFU of WNV isolate 2741 in 20 μl PBS with 5% gelatin. Infected mice were monitored twice daily for morbidity, including lethargy, anorexia and ataxia.

Quantitative PCR (Q-PCR) for determining viral load, T cell levels and cytokine production

Blood, spleen, and brain tissues from control and experimental mice were collected at indicated days post-infection. H36.12j cells (a mouse macrophage cell line) were obtained from the American Type Culture Collection (Manassas, VA) and incubated on 12-well plates (1×10^5 cells/well) for 24h at 37 °C and then infected with WNV (multiplicity of infection = 1). Cells were harvested at day 1 post-infection. Viral RNA was extracted using RNeasy extraction (Qiagen, Valencia, CA). The extracted RNA was eluted in a total volume of 50 sl of RNase-free water. Two hundred fifty nanograms of each extracted RNA sample was used to synthesize cDNA using the ProSTAR First-strand RT-PCR kit (Stratagene, Cedar Creek, TX). The sequences of the primer-probe sets for WNV envelope gene (*WNVE*) and PCR reaction conditions were described previously (5,28). Probes contained a 5′ reporter, FAM, and a 3′ quencher, TAMRA (Applied Biosystems, Foster City, CA). The assay was performed on an iCycler (Bio-Rad, Hercules, CA). The sequences of the primer sets for CD4, CD8, and CXCL10 genes were described in previous publications (10,29). Q-PCR analysis for these genes was performed using RT^2 Real-Time™ SYBR Green/Fluorescein PCR master mix (Superarray, Frederick, MD). To normalize the samples, the same amount of cDNA was used in a Q-PCR for β-actin. The ratio of the amount of amplified gene compared with the amount of *β-actin* *c*DNA represented the relative levels in each sample.

ELISA

Microtiter plates were coated with recombinant WNV-E protein expressed in *Drosophila melanogaster* S2 cells (30) overnight at 4°C at 100 ng/well in coating buffer [0.015 M Na_2CO_3, 0.03 M $NaHCO_3$, and 0.003 M NaN_3 (pH 9.6)]. Sera from infected mice were diluted from 1/40 or 1/100 in PBS with 2% BSA, added to the duplicate wells, and incubated for 1 h at room temperature. Plates were washed three times with PBS-Tween (PBST). Alkaline phosphatase-conjugated goat anti-mouse IgG or IgM (Sigma-Aldrich, St. Louis, MO) at a dilution of 1/1000 in PBS-T was added for 1h at room temperature. After washing three times with PBS-T, color was developed with *p*-nitrophenyl phosphate (Sigma-Aldrich) for 10 min and intensity determined at an absorbance of 405 nm using a spectrophotometer.

Isolation of brain leukocytes

Brain leukocytes were isolated at day 11 post-infection based on a previously described method (31). Prior to harvest, extensive cardiac perfusion was done using PBS to deplete intravascular leukocytes. Brains were collected and homogenized. The cell homogenates were centrifuged and resuspended in 7 ml PBS with 2% fetal bovine serum mixed with 3 ml of 90% percoll (Sigma-Aldrich) in PBS. The suspension was next underlaid with 1 ml of 70% Percoll in RPMI and centrifuged at 800 × g for 20 min at 22°C. Leukocytes at the interface were harvested and counted.

T cell purification from spleen and brain

Single cell suspensions of T cells were made from spleens of WNV-infected mice or brain leukocytes by a positive selection method, using anti-CD90 magnetic beads (Miltenyi Biotec, Auburn, CA) according to the manufacturer's instructions.

In vitro T cell infection and virus titration

Purified splenic T cells were incubated on 96-well plates (2×10^5 cells/well) for overnight at 37 °C and infected with WNV (multiplicity of infection = 0.5) for 1h. Cells were washed after infection and incubated at 37 °C. Supernatant was harvested at days 2, 3 and 5 post-infection. Virus titers were determined by plaque assay. Briefly, Vero cells were seeded in 6-well plates in Dulbecco's modified Eagle's medium (DMEM, Invitrogen, Carlsbad, CA) supplemented with 10% fetal bovine serum (Sigma, St. Louis, MO) 24h before infection. Serial dilutions of

supernatant from infected T cell culture were added and incubated for 1h. Subsequently, DMEM containing 1% low-melting-point agarose was added and the plates were incubated for 4 days. A second overlay of 2.5ml 1% agarose-medium containing 0.01% neutral red was added to visualize plaques. Virus concentrations were determined as PFU/ml.

Flow cytometry

Freshly isolated splenocytes were stained with antibodies specific for CD4, CD8 (BD Biosciences, San Diego, CA) and CXCR3 (R&D, Minneapolis, MN). Isolated brain leukocytes were stained with antibodies for cell surface markers, including CD3, CD4, CD8 and CD45 (BD Biosciences). After staining, cells were fixed with 0.5% paraformaldehyde in PBS and examined using a Coulter XL flow cytometer (Beckman Coulter, Fullerton, CA). Dead cells were excluded on the basis of forward and side light scatter. Data were analyzed using FCS express 2 (De Novo Software Ontario, Canada).

Intracellular cytokine staining

To measure cytokine production, splenocytes from WNV-infected mice were isolated and then stimulated at 2.5×10^6 cells/ml with 50 ng/ml PMA (Sigma-Aldrich) and 500 ng/ml ionomycin (Sigma-Aldrich) for 5 h at 37°C. Golgi-plug (BD Biosciences) was added during the final 3.5h. The cells were then harvested, stained with antibodies (BD Biosciences) for TCRαβ and CD8α and fixed in 2% paraformaldehyde. The cells were then permeabilized with 0.5% saponin before adding Phycoerythrin (PE)-conjugated anti-IFN-γ (clone XMG 1.2) or control PE-conjugated rat IgG_1 (BD Biosciences). Cells were analyzed using a Coulter XL instrument as described above.

Cytometric bead array (CBA)

At days 2 and 4 post-infection, sera were collected from mice and measured for IFN-γ production using a mouse Th1/Th2 cytokine kit (BD Biosciences, which includes assays for IL-2, IL-4, IL-5, IFN-γ, and TNF-α) using a FACSArray analyzer (BD Biosciences).

Immunofluorescence microscopy

Mice were transcardially perfused with PBS, and brains were placed in 4% paraformaldehyde in PBS overnight at 4 °C, and, in the case of cryoimmunohistochemistry, cryoprotected with 10% (w/v) followed by 20% (w/v) and then 30% (w/v) sucrose in PBS for 24h each before embedding in Optimal Cutting Temperature compound. Subsequently, specimens were processed and histological slides were prepared for staining with various antibodies. For paraffin sections, we processed antigen retrieval at 90°C for 30 min in 10% (v/v) target retrieval solution (Dakocytomation, Denmark) or by treatment with 88% formic acid for 8 min. The endogenous peroxidase activity was quenched in 0.3% H_2O_2 for 30 min at room temperature. We performed the staining using the Vectastain *Elite* ABC kit coupled to the 3′-3 diaminobenzadine substrate (Vector Laboratories, Burlingame, CA). Rat antibody specific for mouse CD45 (clone YW 62.3, Serotec, Raleigh, NC), or mouse ascitic fluid WNV antibodies were used. Sections were digitized with Kodak scientific imaging software (Eastman Kodak, Rochester, NY). For splenic and brain T cell staining, 80,000 cells were fixed by submerging them in acetone at −20°C for 30 min. Cells were stained and antigens detected with PE-Cy5 conjugated antibodies to CD8 or CD4 and the flavivirus E protein-specific monoclonal antibody 4G2 ((32), 1:150 dilution) for 1.5 h at 37°C followed by biotinylated anti-mouse IgG (1:200 dilution) for 1.5 h and streptavidin-fluorescein isothiocyanate (GE Healthcare Bio-Sciences Corp., Piscataway, NJ) for 30 min at 37°C.

Statistical analysis

Survival curve comparisons were performed using Prism software (GraphPad Software, San Diego, CA) statistical analysis, which uses the log rank test (equivalent to the Mantel-Haenszel test). Values of *p* for viral burden, cytokine production, antibody titer and T cell number experiments were calculated with a non-paired Student's t test or Mann-Whitney test.

Results

Drak2$^{-/-}$ mice are more resistant to WNV infection

Drak2$^{-/-}$ mice were previously shown to be more resistant to EAE than wild-type mice due, in part to a decrease in the number of cells infiltrating the CNS (26). WNV infection also induces the migration of lymphocytes into the CNS (10,18). In order to examine if Drak2 is involved in WNV-induced encephalitis, we challenged *Drak2*$^{-/-}$ mice and wild-type mice intraperitoneally i.p. with 800 p.f.u. of WNV and monitored the mice twice daily for survival. *Drak2*$^{-/-}$ mice were more resistant (47% survival) to lethal WNV infection than wild-type controls (16.7% survival) (Fig. 1**,** $P < 0.05$). Throughout infection, the kinetics and magnitude of viremia in *Drak2*$^{-/-}$ mice were not significantly different from that of wild-type controls (Fig. 2*A*, $P > 0.05$). Although viral load was slightly reduced in spleens of *Drak2*$^{-/-}$ mice at day 2 (Fig. 2*B*, $P < 0.05$), no difference was noted between these two groups at the later stage of viral infection (days 4 and 6, $P > 0.05$). Nevertheless, there was a nearly sixty-fold reduction in viral load in the brains of *Drak2*$^{-/-}$ mice at day 6 (peak of infection in the brain) and seven to eightfold reduction at day 9 following WNV challenge (Fig. 2*C*, $P < 0.05$). These data suggest that Drak2 plays a role in the lethality and affects the virus levels in the CNS following WNV challenge.

Humoral responses remain normal in Drak2$^{-/-}$ mice upon WNV infection

Drak2 is specifically expressed in T and B cells (26). B cell-mediated humoral immune responses are critical for the host defense against disseminated infection by WNV (14,33). Therefore, we next measured WNV-specific IgM and IgG levels in the sera from *Drak2*$^{-/-}$ and wild-type mice following primary WNV infection. At days 5 and 9 post-infection, we did not detect significant differences between the two groups in regard to either the IgM or IgG response (Figs. 3*A* & 3*B*, $P > 0.05$). These data suggest that the absence of Drak2 does not influence the development of antibody following WNV infection.

There are more IFN-γ-producing splenocytes from Drak2$^{-/-}$ mice after ex vivo stimulation

Cellular immunity plays an important role in host survival during WNV infection (8,13). To understand the role of Drak2 in regulating peripheral T cell responses during WNV infection, we analyzed IFN-γ production of splenic CD4$^+$ and CD8$^+$ T cells from WNV infected mice using an *ex vivo* intracellular cytokine assay. As shown in Fig. 4*A*, at day 5 post-infection, more splenic CD4$^+$ T cells in *Drak2*$^{-/-}$ mice produced IFN-γ upon *ex vivo* stimulation with PMA and ionomycin than those of wild-type mice, while there was not a difference in the number of IFN-γ-producing CD8$^+$ T cells at this time. However, at day 9 post-infection, there was a two-fold increase in the number of CD4$^+$ and CD8$^+$ T cells that produced IFN-γ in *Drak2*$^{-/-}$ mice compared to wild-type mice (Fig. 4*A*). These results suggest that *Drak2*$^{-/-}$ T cells respond to WNV infection; in fact, there is an increase in the number of cells that produce IFN-γ upon *ex vivo* stimulation compared to wild-type mice during WNV infection. Surprisingly, we noted no significant differences in production of IFN-γ (Fig. 4*B*, $P < 0.05$) or other Th1/Th2 cytokines (data not shown here) in sera of these two groups of mice at days 2 and 4 post-infection.

There are fewer Drak2$^{-/-}$ T cells in the brain following WNV infection

In the EAE model, *Drak2*$^{-/-}$ mice exhibited a reduced number of infiltrating cells in the spinal cord (26), suggesting a role for Drak2 in T cell infiltration into the CNS. A hallmark of WNV encephalitis is the accumulation of inflammatory infiltrates, which reportedly varies between brain regions and consists predominantly of lymphocytes and macrophages (10). Thus, to study T cell infiltration into the CNS, we first measured CD4$^+$ and CD8$^+$ T cell levels in the brain by Q-PCR analysis. In the brains of *Drak2*$^{-/-}$ mice, we observed more than a two-fold reduction of CD4$^+$ T cells (Fig 5*A*, left panel) at day 9 post-infection and at least a two-fold reduction of CD8$^+$ T cells (Fig. 5*A*, right panel) at days 6 and 9 post-infection, compared to wild-type mice. To verify these results, we isolated brain leukocytes at day 11 post-infection. As shown in Fig. 5*B*, the percentage of CD3$^+$CD4$^+$ T cells in the brains of *Drak2*$^{-/-}$ mice was lower than in those of wild-type mice (2.8% vs. 7.3%, *Drak2*$^{-/-}$ vs. wild-type). The percentage of CD3$^+$CD8$^+$ among *Drak2*$^{-/-}$ mice brain leukocytes was also reduced (7.0% vs. 19%, *Drak2*$^{-/-}$vs. wild-type). The total number of CD4$^+$ and CD8$^+$ T cells in the brains of *Drak2*$^{-/-}$ mice was also more than two-fold lower compared to wild-type mice (Fig. 5*D*, $P < 0.05$). Consistent with these results, the percentage of CD45$^+$ CD3$^+$ leukocytes in *Drak2*$^{-/-}$ mouse brains was lower than in those of wild-type mice (Fig. 5*C*). Interestingly, no differences were noted when we compared the number of CD45$^+$CD3$^-$ cells in the brains of *Drak2*$^{-/-}$ mice and wild-type mice (Fig. 5*D*). These results further suggest that Drak2 is important for T cell infiltration into the CNS upon WNV infection.

T cells are potential carriers for WNV entry into the CNS

Earlier Q-PCR analyses revealed a significantly reduced viral load in *Drak2*$^{-/-}$ mice brains at days 6 and 9 following WNV challenge (Fig. 2*C*). At day 13 post-infection, immunofluorescence double-staining of wild-type mouse brains (olfactory bulbs, cerebellum and brain stem) showed either numerous CD45$^+$ leukocytes (Fig. 6*A*) or CD4$^+$ T cells (Fig. 6*B*) in the vicinity of WNV-positive cells, but in the same regions of *Drak2*$^{-/-}$ mouse brains the staining of both WNV antigen and T cells was less obvious. These data indicate that reduced T cell migration into the CNS is correlated with decreased viral levels in the brains. To test whether non-T cells in the CNS contribute to difference of susceptibility to WNV infection between wild-type and *Drak2*$^{-/-}$mice, we next infected mice i.c. with 160PFU WNV isolate 2741. As shown in Fig. 6*C*, viral load in the brains of *Drak2*$^{-/-}$ mice was not significantly different from that of wild-type controls around the peak of infection (day 5) ($P > 0.05$). Therefore, it is possible that WNV enters the CNS through infiltrating T cells. To test this possibility, we determined whether peripheral T cells were permissive to WNV infection. Following i.p. challenge, splenic T cells were isolated at day 6 post-infection. The purity of these cells was close to 90% as analyzed by flow cytometry (Fig. 7*A*). Q-PCR analysis for viral load of the purified T cells revealed a similar level of infection as the day 1 WNV infected H36.12j cells (Fig. 7*B*). Immunofluorescence staining (Fig. 7*C*) also demonstrated WNV antigens in these cells. Further, we isolated brain-infiltrating T cells from wild-type mice at day 10 post-infection and stained for WNV antigen and CD4 or CD8 T cell markers. Immunofluorescence double-staining shows CD4$^+$WNV$^+$ and CD8$^+$WNV$^+$ populations in these purified brain T cells (Fig 7*D*). Plaque assay showed WNV replicated productively in purified splenic T cells from both groups of mice at day 2 and 3 post-infection, but decreased at day 5, suggesting *Drak2*$^{-/-}$ T cells supporting a short-term productive virus replication as efficiently as wild-type T cells (Fig. 7*E*). Overall, these results indicate that infected T cells might carry WNV as they migrate into the brains, thereby serving as one of the pathways for WNV entry into the CNS.

Drak2 affects chemokine expression during WNV infection

Interactions between chemokines and their receptors is an important step in the control of leukocyte migration into sites of inflammation. Neurons are the primary target for WNV in the CNS (23). Infected neurons secrete chemokines, such as CXCL10, which recruits effector T cells via the chemokine receptor CXCR3 (31) (10). To investigate whether Drak2 plays a role in chemokine signaling, we analyzed CXCL10 levels in the brain following WNV infection. At day 4 post-infection, there was a two-fold reduction of CXCL10 mRNA in the brain of *Drak2*$^{-/-}$mice as measured by Q-PCR. This difference was more dramatic at day 6 post-infection (Fig 8*A*). In addition, we found that the percentage of splenic CD8^{+} T cells expressing CXCR3 was slightly lower in *Drak2*$^{-/-}$ mice than wild-type mice at day 5 post-infection; whereas the percentage of CD4^{+} T cells expressing CXCR3 did not differ in mice of these two groups (Fig. 8*B* left panel). Furthermore, the total numbers of CD4^{+} T cells ($20.7 \pm 1.2 \times 10^6$ vs. $13.9 \pm 0.5 \times 10^6$, wild-type vs. *Drak2*$^{-/-}$, $P < 0.05$) and CD8^{+} T cells ($15.6 \pm 0.8 \times 10^6$ vs. $9.8 \pm 0.8 \times 10^6$, wild-type vs. *Drak2*$^{-/-}$, $P < 0.05$) were higher in wild-type mice than those of *Drak2*$^{-/-}$ mice. The total numbers of CD4^{+} and CD8^{+} spleen T cells expressing CXCR3 were also higher in wild-type mice than in *Drak2*$^{-/-}$ mice (Fig. 8*B* right panel).

Discussion

The mechanism(s) by which WNV evades the immune system in susceptible organisms and enters the CNS is not completely understood. In this study, we have investigated the role of Drak2 in WNV-induced encephalitis. We demonstrated that *Drak2*$^{-/-}$ mice were more resistant to lethal WNV infection than wild-type controls. In the peripheral tissues, virus infection was not significantly different between wild-type and *Drak2*$^{-/-}$ mice. A defect in Drak2 signaling did not affect the development of antibodies following WNV infection. Although more *Drak2*$^{-/-}$ T cells isolated from WNV-infected mice produced IFN-γ upon *ex vivo* stimulation, no significant difference in IFN-γ production was found in the sera of mice in these two groups at days 2 and 4 post-infection. These data indicate that Drak2 is not involved in the control of virus dissemination in the peripheral tissues. Nevertheless, we noted a drastically reduced viral load in the brains of *Drak2*$^{-/-}$ mice, compared to that in wild-type controls. Interestingly, there was also a reduction in CD4^{+} and CD8^{+} T cell infiltrates in the brains of *Drak2*$^{-/-}$ mice. Together, these results indicate a correlation between the number of T cells in the brain and virus dissemination in this organ. Moreover, we demonstrated that upon WNV challenge, T cells from either a peripheral organ or from brain infiltrates contained WNV antigens. Overall, our data suggest that Drak2 is important for maintaining CD4^{+} and CD8^{+} T cells in the CNS following a systemic WNV challenge, and may also be involved in WNV entry into the CNS.

There are several possible explanations for the reduction of T cells in the brain of *Drak2*$^{-/-}$ mice. One possibility is that Drak2 is required for T cell migration into the CNS. However, a recent report by Ramos et al. (34) revealed that *Drak2*$^{-/-}$ T cells migrate to the brain following mouse hepatitis virus (MHV) infection. However, in this experiment, the virus was injected directly into the brain, and the migration of T cells into the CNS may be mediated by different mechanisms when physical trauma is induced. Nevertheless, when *Drak2*$^{-/-}$ mice were infected i.p. with lymphocytic choriomeningitis virus (LCMV), a similar number of T cells were present in the brain compared to wildtype mice early after infection. However, by thirteen days post-infection, there were fewer T cells in the brain of *Drak2*$^{-/-}$ mice, and of the T cells that were present, a higher percent were undergoing apoptosis (McGargill MA, and Hedrick SM. et. al. Manuscript submitted). Likewise, during EAE, there were similar numbers of *Drak2*$^{-/-}$ and wild-type T cells early after the induction of disease, however the *Drak2*$^{-/-}$ T cells were more sensitive to apoptosis, and therefore did not accumulate and induce disease similar to the wild-type T cells. These data suggest that T cells can migrate to the CNS in the absence of *Drak2*, however, the cells are more sensitive to death, and therefore do not remain

in this organ. Although, we did detect a difference in chemokine expression in the brain, and a slight reduction in chemokine receptor on T cells, this may be secondary to the fact that the T cells do not remain in the brain in the absence of *Drak2*. It is possible that after systemic WNV infection, T cells carry virus into the brain, which results in the infection of neurons and upregulation of CXCL10, and in turn, amplifies the recruitment of T cells to the CNS. However, in *Drak2*$^{-/-}$ mice, T cells do not remain in the CNS, which may limit the opportunity of virus to spread to the neurons, and therefore there is not an upregulation of chemokines. It is interesting to speculate whether there are fewer T cells in the CNS of *Drak2*$^{-/-}$ mice due to a decrease in viral antigen in the brain, or whether there is a decrease in viral antigen in the CNS as a result of the reduction of T cells in this organ. Regardless, there is a decrease in WNV-induced lethality in the absence of *Drak2*, which is likely due to both the decrease of T cells and viral load in the CNS.

Recent studies have shown that WNV-induced proinflammatory responses could modulate BBB permeability, which might enable viral entry into and infection of the brain, leading to induction of lethal encephalitis (5,21). As a result, mice which are deficient in proinflammatory cytokine signaling, including macrophage migration inhibitory factor and tumor necrosis factor-alpha receptor 1, have a reduced viral load in the brain and are subsequently more resistant to lethal WNV infection (5,21). Following BBB compromise, WNV may enter the CNS via one or more pathways. The virus may invade the CNS by crossing the BBB directly (20,35) or by being carried into the brain by infected infiltrating myeloid cells (36,37) and inducing encephalitis. In this study, we have shown that the absence of *Drak2* attenuates lethality from WNV encephalitis by 30%, and this is accompanied by a decrease of T cells in the CNS.

The role of T cells in protecting the host against WNV infection has been the subject of recent investigations. Both αβ and γδ T cells have been shown to contribute to host survival during WNV infection (8,13). Among αβ T cells, CD4$^+$ T cells respond vigorously in the periphery (16), whereas CD8$^+$ T cell responses have been observed in both the spleen and brain following WNV infection (38). CD4$^+$ T cells are known to provide help for antibody responses and to sustain WNV-specific CD8$^+$ T cell responses in the CNS enabling viral clearance (39). CD8$^+$ T cells have important functions in clearing infection from peripheral tissues and CNS, and in preventing viral persistence (40,41). Further, FasL effector or perforin-dependent mechanisms (17,42) are critical for CD8$^+$ T cells to clear WNV infection in the CNS. CD40-CD40L interactions have also been demonstrated to be important for T cell trafficking into the CNS and for protection of the host from a low dose WNV challenge (43).

Immune responses are also involved in viral pathogenesis. For example, one study has shown that CD8$^+$ T cells contribute to immunopathology upon high-dose WNV challenge (18). Nevertheless, little is known about the role of T cell-mediated pathology in WNV-related brain damage. Our data now provide the first evidence that Drak2-mediated T cell survival in the CNS plays an important role in WNV pathogenesis. These results may prompt the development of new pharmacotherapeutic treatment using Drak2 signaling inhibitors, alone or in combination with currently existing antiviral agents, in treating encephalitis caused by WNV and perhaps, other viral encephalitides.

Acknowledgements

We thank Dr. Richard Bowen for performance of i.c. injection with WNV, Matt Whitney for technical assistance, and Drs. Alan Schenkel and Brian Foy for help with immunofluorescence microscope studies. We also thank Dr. Charlie Calisher for critical reading of the manuscript.

This work was supported by NIH grant to S.M.H. (AI053091) and a grant to T.W. from Colorado State University. T. T. is supported by an Alzheimer's Association grant and an NIH/NIA "Pathway to Independence" award

(1K99AG029726-01). E.F., R.A.F. and T.W. are supported by NIH grants AI055749, AI50031 and AI072060. R.A.F. and E.F. are Investigators of the Howard Hughes Medical Institute.

References

1. Campbell GL, Marfin AA, Lanciotti RS, Gubler DJ. West Nile virus. Lancet Infect Dis 2002;2:519–529. [PubMed: 12206968]
2. Pletnev AG, Swayne DE, Speicher J, Rumyantsev AA, Murphy BR. Chimeric West Nile/dengue virus vaccine candidate: Preclinical evaluation in mice, geese and monkeys for safety and immunogenicity. Vaccine 2006;24:6392–6404. [PubMed: 16831498]
3. Griffin DE. Arboviruses and the central nervous system. Springer Semin Immunopathol 1995;17:121–132. [PubMed: 8571164]
4. Samuel MA, Wang H, Siddharthan V, Morrey JD, Diamond MS. Axonal transport mediates West Nile virus entry into the central nervous system and induces acute flaccid paralysis. Proc Natl Acad Sci U S A 2007;104:17140–17145. [PubMed: 17939996]
5. Wang T, Town T, Alexopoulou L, Anderson JF, Fikrig E, Flavell RA. Toll-like receptor 3 mediates West Nile virus entry into the brain causing lethal encephalitis. Nat Med 2004;10:1366–1373. [PubMed: 15558055]
6. Diamond MS, Shrestha B, Mehlhop E, Sitati E, Engle M. Innate and adaptive immune responses determine protection against disseminated infection by West Nile encephalitis virus. Viral Immunol 2003;16:259–278. [PubMed: 14583143]
7. Samuel MA, Diamond MS. Pathogenesis of West Nile Virus infection: a balance between virulence, innate and adaptive immunity, and viral evasion. J Virol 2006;80:9349–9360. [PubMed: 16973541]
8. Wang T, Fikrig E. Immunity to West Nile virus. Curr Opin Immunol 2004;16:519–523. [PubMed: 15245749]
9. Fredericksen BL, Keller BC, Fornek J, Katze MG, Gale M Jr. Establishment and maintenance of the innate antiviral response to West Nile Virus involves both RIG-I and MDA5 signaling through IPS-1. J Virol 2008;82:609–616. [PubMed: 17977974]
10. Klein RS, Lin E, Zhang B, Luster AD, Tollett J, Samuel MA, Engle M, Diamond MS. Neuronal CXCL10 directs CD8+ T-cell recruitment and control of West Nile virus encephalitis. J Virol 2005;79:11457–11466. [PubMed: 16103196]
11. Anderson JF, Rahal JJ. Efficacy of interferon alpha-2b and ribavirin against West Nile virus *in vitro*. Emerg Infect Dis 2002;8:107–108. [PubMed: 11749765]
12. Lucas M, Mashimo T, Frenkiel MP, Simon-Chazottes D, Montagutelli X, Ceccaldi PE, Guenet JL, Despres P. Infection of mouse neurones by West Nile virus is modulated by the interferon-inducible 2′-5′ oligoadenylate synthetase 1b protein. Immunol Cell Biol 2003;81:230–236. [PubMed: 12752688]
13. Wang T, Scully E, Yin Z, Kim JH, Wang S, Yan J, Mamula M, Anderson JF, Craft J, Fikrig E. IFN-gamma-producing gammadelta T cells help control murine West Nile virus infection. J Immunol 2003;171:2524–2531. [PubMed: 12928402]
14. Diamond MS, Shrestha B, Marri A, Mahan D, Engle M. B cells and antibody play critical roles in the immediate defense of disseminated infection by West Nile encephalitis virus. J Virol 2003;77:2578–2586. [PubMed: 12551996]
15. Roehrig JT, Staudinger LA, Hunt AR, Mathews JH, Blair CD. Antibody prophylaxis and therapy for flavivirus encephalitis infections. Ann N Y Acad Sci 2001;951:286–297. [PubMed: 11797785]
16. Kulkarni AB, Mullbacher A, Blanden RV. Functional analysis of macrophages, B cells and splenic dendritic cells as antigen-presenting cells in West Nile virus-specific murine T lymphocyte proliferation. Immunol Cell Biol 1991;69(Pt 2):71–80. [PubMed: 1680803]
17. Shrestha B, Samuel MA, Diamond MS. CD8+ T Cells Require Perforin To Clear West Nile Virus from Infected Neurons. J Virol 2006;80:119–129. [PubMed: 16352536]
18. Wang Y, Lobigs M, Lee E, Mullbacher A. CD8+ T cells mediate recovery and immunopathology in West Nile virus encephalitis. J Virol 2003;77:13323–13334. [PubMed: 14645588]

19. Ben-Nathan D, Huitinga I, Lustig S, van Rooijen N, Kobiler D. West Nile virus neuroinvasion and encephalitis induced by macrophage depletion in mice. Arch Virol 1996;141:459–469. [PubMed: 8645088]
20. Halevy M, Akov Y, Ben-Nathan D, Kobiler D, Lachmi B, Lustig S. Loss of active neuroinvasiveness in attenuated strains of West Nile virus: pathogenicity in immunocompetent and SCID mice. Arch Virol 1994;137:355–370. [PubMed: 7944955]
21. Arjona A, Foellmer HG, Town T, Leng L, McDonald C, Wang T, Wong SJ, Montgomery RR, Fikrig E, Bucala R. Abrogation of macrophage migration inhibitory factor decreases West Nile virus lethality by limiting viral neuroinvasion. J Clin Invest 2007;117:3059–3066. [PubMed: 17909632]
22. Sampson BA, Armbrustmacher V. West Nile encephalitis: the neuropathology of four fatalities. Ann N Y Acad Sci 2001;951:172–178. [PubMed: 11797775]
23. Shrestha B, Gottlieb D, Diamond MS. Infection and injury of neurons by West Nile encephalitis virus. J Virol 2003;77:13203–13213. [PubMed: 14645577]
24. Xiao SY, Guzman H, Zhang H, Travassos da Rosa AP, Tesh RB. West Nile virus infection in the golden hamster (Mesocricetus auratus): a model for West Nile encephalitis. Emerg Infect Dis 2001;7:714–721. [PubMed: 11585537]
25. Kogel D, Prehn JH, Scheidtmann KH. The DAP kinase family of pro-apoptotic proteins: novel players in the apoptotic game. Bioessays 2001;23:352–358. [PubMed: 11268041]
26. McGargill MA, Wen BG, Walsh CM, Hedrick SM. A deficiency in Drak2 results in a T cell hypersensitivity and an unexpected resistance to autoimmunity. Immunity 2004;21:781–791. [PubMed: 15589167]
27. Friedrich ML, Cui M, Hernandez JB, Weist BM, Andersen HM, Zhang X, Huang L, Walsh CM. Modulation of DRAK2 autophosphorylation by antigen receptor signaling in primary lymphocytes. J Biol Chem 2007;282:4573–4584. [PubMed: 17182616]
28. Lanciotti RS, Kerst AJ, Nasci RS, Godsey MS, Mitchell CJ, Savage HM, Komar N, Panella NA, Allen BC, Volpe KE, Davis BS, Roehrig JT. Rapid detection of West Nile virus from human clinical specimens, field- collected mosquitoes, and avian samples by a TaqMan reverse transcriptase-PCR assay. J Clin Microbiol 2000;38:4066–4071. [PubMed: 11060069]
29. Phares TW, Kean RB, Mikheeva T, Hooper DC. Regional differences in blood-brain barrier permeability changes and inflammation in the apathogenic clearance of virus from the central nervous system. J Immunol 2006;176:7666–7675. [PubMed: 16751414]
30. Wong SJ V, Demarest L, Boyle RH, Wang T, Ledizet M, Kar K, Kramer LD, Fikrig E, Koski RA. Detection of human anti-flavivirus antibodies with a West Nile virus recombinant antigen microsphere immunoassay. J Clin Microbiol 2004;42:65–72. [PubMed: 14715733]
31. Glass WG, Lim JK, Cholera R, Pletnev AG, Gao JL, Murphy PM. Chemokine receptor CCR5 promotes leukocyte trafficking to the brain and survival in West Nile virus infection. J Exp Med 2005;202:1087–1098. [PubMed: 16230476]
32. Davis BS, Chang GJ, Cropp B, Roehrig JT, Martin DA, Mitchell CJ, Bowen R, Bunning ML. West Nile virus recombinant DNA vaccine protects mouse and horse from virus challenge and expresses in vitro a noninfectious recombinant antigen that can be used in enzyme-linked immunosorbent assays. J Virol 2001;75:4040–4047. [PubMed: 11287553]
33. Diamond MS, Sitati EM, Friend LD, Higgs S, Shrestha B, Engle M. A critical role for induced IgM in the protection against West Nile virus infection. J Exp Med 2003;198:1853–1862. [PubMed: 14662909]
34. Ramos SJ, Hardison JL, Stiles LN, Lane TE, Walsh CM. Anti-viral effector T cell responses and trafficking are not dependent upon DRAK2 signaling following viral infection of the central nervous system. Autoimmunity 2007;40:54–65. [PubMed: 17364498]
35. Lustig S, Danenberg HD, Kafri Y, Kobiler D, Ben-Nathan D. Viral neuroinvasion and encephalitis induced by lipopolysaccharide and its mediators. J Exp Med 1992;176:707–712. [PubMed: 1512538]
36. Cardosa MJ, Porterfield JS, Gordon S. Complement receptor mediates enhanced flavivirus replication in macrophages. J Exp Med 1983;158:258–263. [PubMed: 6864163]
37. Gollins SW, Porterfield JS. Flavivirus infection enhancement in macrophages: an electron microscopic study of viral cellular entry. J Gen Virol 1985;66(Pt 9):1969–1982. [PubMed: 4031825]

38. Liu Y, Blanden RV, Mullbacher A. Identification of cytolytic lymphocytes in West Nile virus-infected murine central nervous system. J Gen Virol 1989;70:565–573. [PubMed: 2543751]

39. Sitati EM, Diamond MS. CD4+ T-cell responses are required for clearance of West Nile virus from the central nervous system. J Virol 2006;80:12060–12069. [PubMed: 17035323]

40. Brien JD, Uhrlaub JL, Nikolich-Zugich J. Protective capacity and epitope specificity of CD8(+) T cells responding to lethal West Nile virus infection. Eur J Immunol 2007;37:1855–1863. [PubMed: 17559175]

41. Shrestha B, Diamond MS. Role of CD8+ T cells in control of West Nile virus infection. J Virol 2004;78:8312–8321. [PubMed: 15254203]

42. Shrestha B, Diamond MS. Fas ligand interactions contribute to CD8+ T-cell-mediated control of West Nile virus infection in the central nervous system. J Virol 2007;81:11749–11757. [PubMed: 17804505]

43. Purtha WE, Myers N, Mitaksov V, Sitati E, Connolly J, Fremont DH, Hansen TH, Diamond MS. Antigen-specific cytotoxic T lymphocytes protect against lethal West Nile virus encephalitis. Eur J Immunol 2007;37:1845–1854. [PubMed: 17559174]

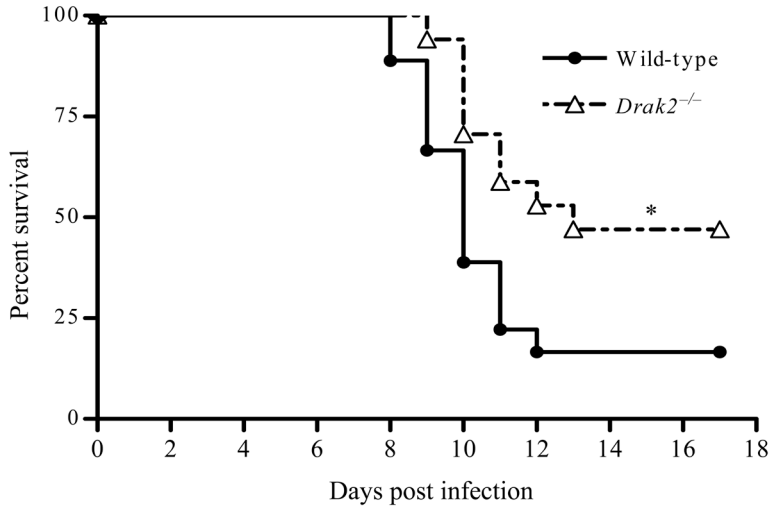

Figure 1.

Drak2$^{-/-}$ mice are more resistant to lethal WNV infection. Wild-type and *Drak2*$^{-/-}$ mice were infected with a dose close to an LD_{100} of WNV and monitored twice daily for mortality. Data shown are pooled from three independent experiments. $P = 0.02 < 0.05$ for wild-type ($n = 18$) vs. *Drak2*$^{-/-}$ mice ($n = 17$).

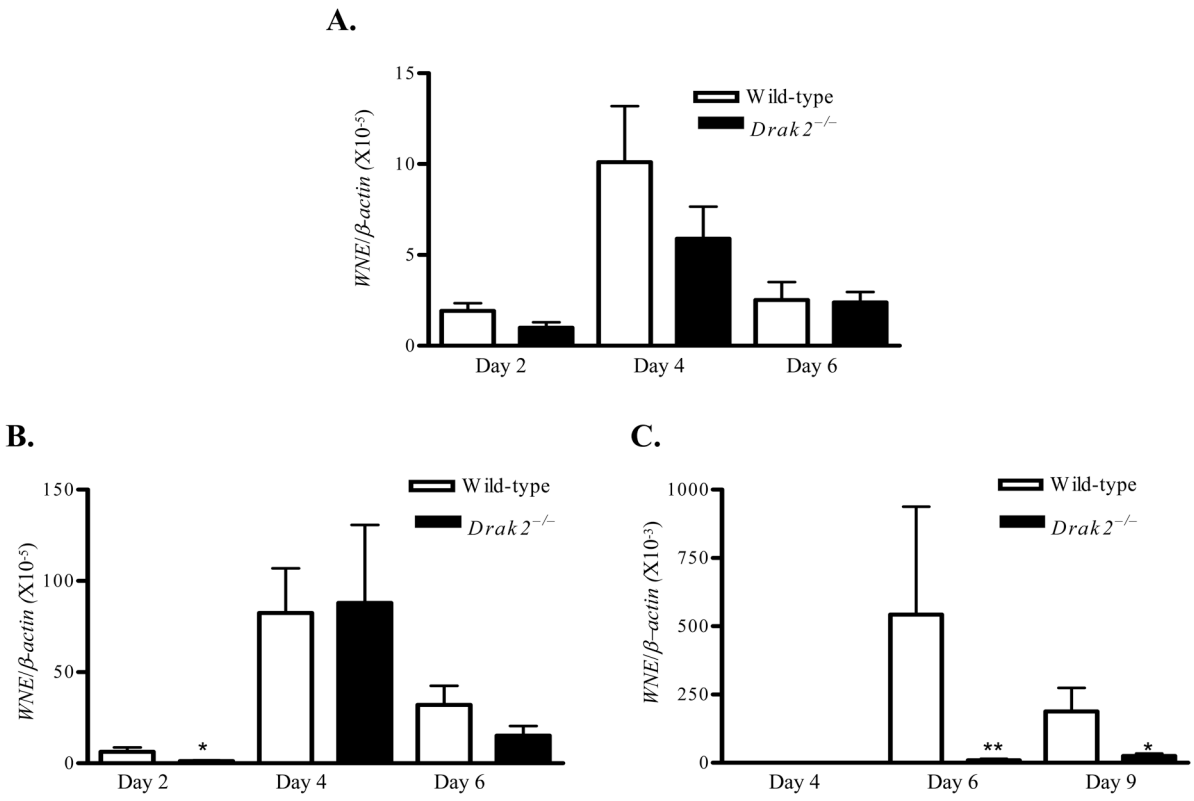

Figure 2.

Viral load analysis in wild-type and *Drak2*$^{-/-}$ mice. Viral load was determined in blood (*A*), spleen (*B*), and brain (*C*) of wild-type and *Drak2*$^{-/-}$ mice at the indicated days following WNV infection using Q-PCR. The y-axis depicts the ratio of the amplified *WNV-E* cDNA to *β-actin* cDNA of each sample (unitless ratio ± SEM). 5–8 samples were collected at each condition. $P < 0.05$ compared to wild-type mice. Data shown were representative of two independent experiments.

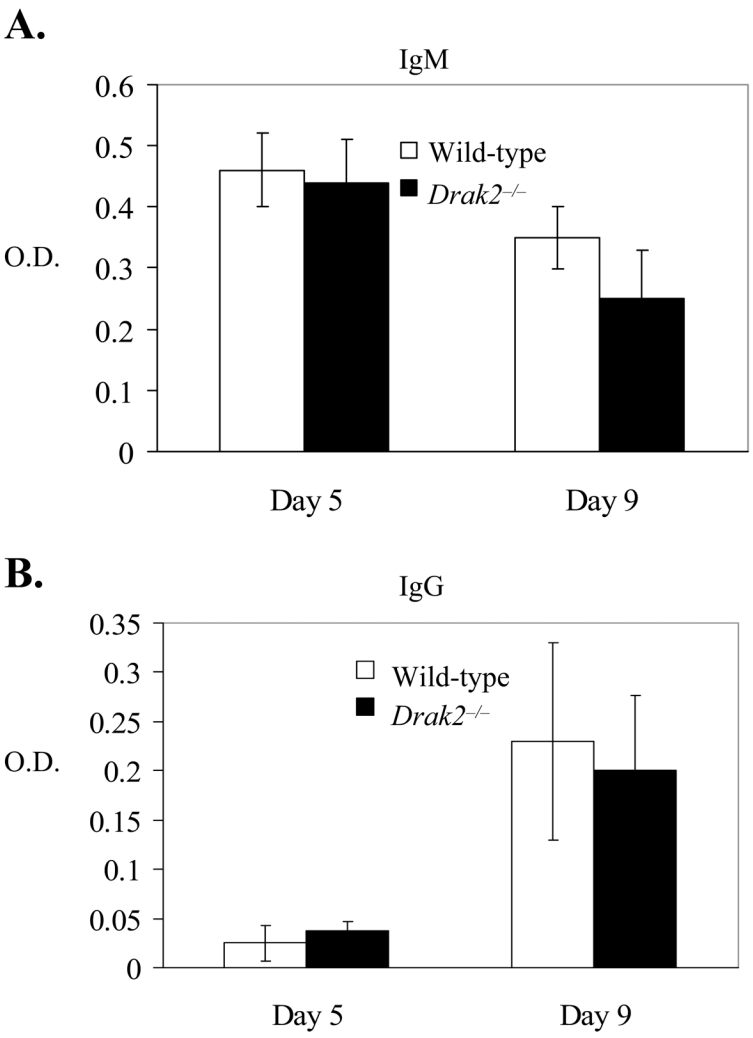

Figure 3.

Humoral responses remain normal in *Drak2*$^{-/-}$ mice upon WNV infection. Sera were collected from wild-type or *Drak2*$^{-/-}$ mice at the indicated days during WNV infection. The development of specific IgM (*A*) or IgG (*B*) antibodies to WNV was determined after incubating sera with absorbed purified r-WNV-E protein. Data shown are representative of three similar experiments and are the average of four mice in each experiment per time point, performed in duplicate.

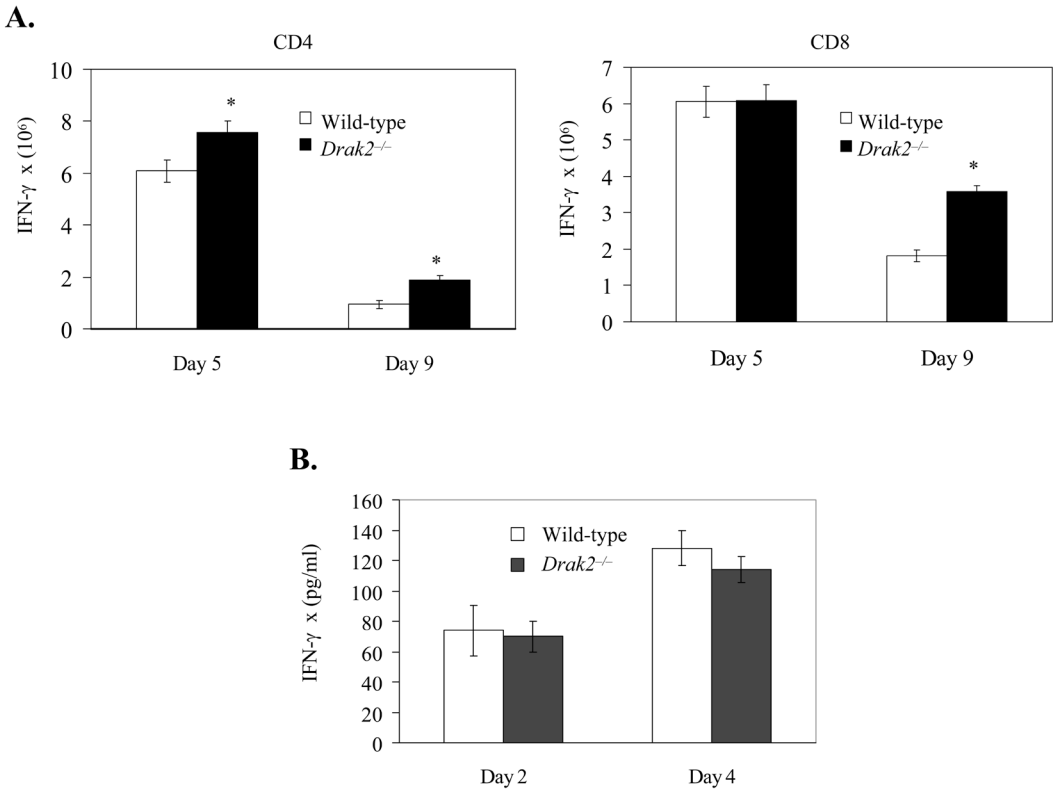

Figure 4.

IFN-γ production in wild-type and *Drak2*$^{-/-}$ mice following WNV infection. *A*, Splenocytes were isolated from WNV-infected wild-type and *Drak2*$^{-/-}$ mice (4 samples per condition) at days 5 and 9 post-infection and were cultured *ex vivo* with PMA plus ionomycin, as described in Materials and Methods, and stained for IFN-γ, CD4 or CD8. Total number of IFNγ^{+}CD4^{+} (left panel) and IFNγ^{+}CD8^{+} (right panel) is shown. Data presented are representative of two similar experiments. $P < 0.05$ compared to wild-type mice. *B*, Sera were collected from wild-type or *Drak2*$^{-/-}$ mice at the indicated days during WNV infection. IFN-γ production was measured using mouse Th1/Th2 cytokine kit. Data shown are representative of two independent experiments and are the average of four mice in each experiment per time point.

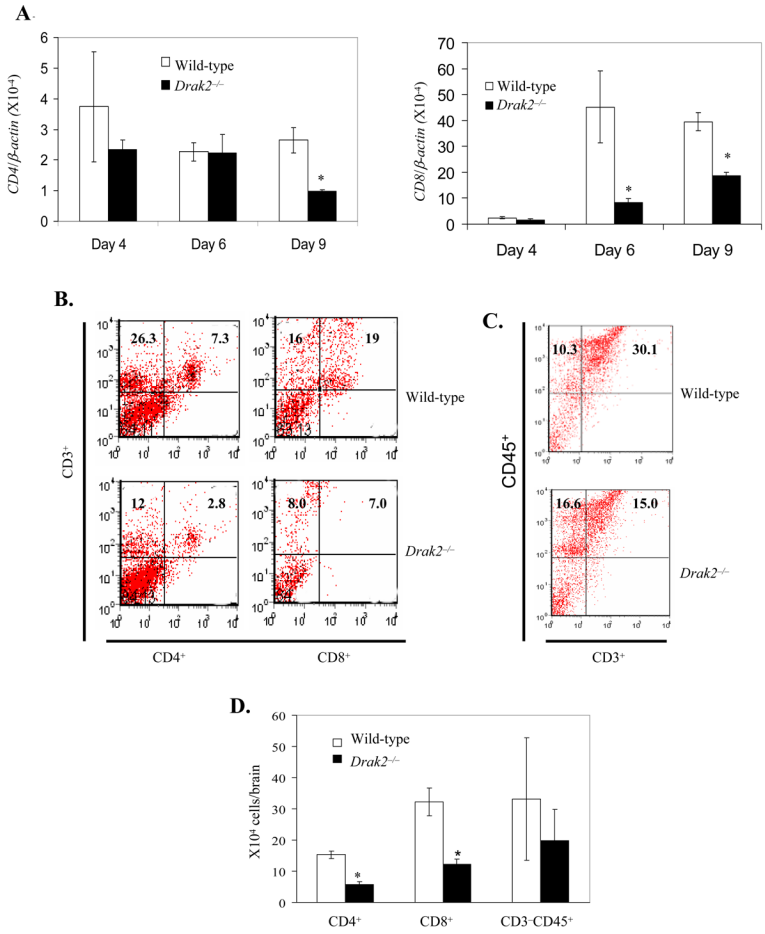

Figure 5.

There are fewer *Drak2*$^{-/-}$ T cells in the CNS following systemic WNV infection. *A*, CD4 (left panel) and CD8 levels (right panel) in WNV infected mice brains were measured by Q-PCR at indicated days. The y-axis depicts the ratio of the amplified *CD4* or *CD8*-cDNA to *β-actin* cDNA of each sample (unitless ratio ± SEM). $P < 0.05$ compared to wild-type mice. Data shown are one representative of three independent experiments. Four samples were collected from each condition. (*B*) & (*D*), Numeric reduction of CD4$^+$ and CD8$^+$ T cells in the brains of wild-type and *Drak2*$^{-/-}$ mice at day 11 post-infection. (*C*) & (*D*), Number of CD45$^+$CD3$^-$ cells in the brains of *Drak2*$^{-/-}$ mice and wild-type mice was not different. At least three samples were collected at each condition. Experiments were repeated four times.

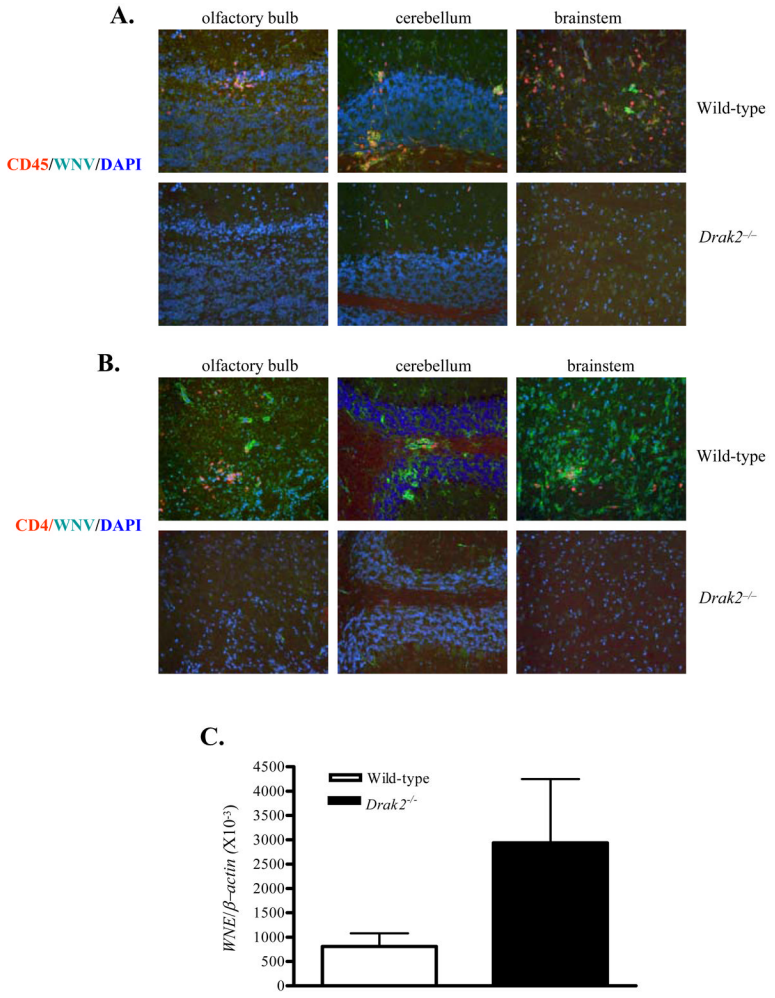

Figure 6.

T cell migration into the CNS is correlated with enhanced viral load in the brains following systemic WNV infection. *A* & *B*, Wild-type (n = 4) and *Drak2*$^{-/-}$ mice (n = 4) mice were infected with WNV, brains were isolated at day 13 post-infection, and immunostained with antibodies against CD45 (*A*, red signal) or CD4 (*B*, red signal) and WNV antigen (green signal) to reveal infiltrating leukocytes or T cells in WNV infected brain regions (olfactory bulbs, cerebellum, and brain stem sections). DAPI was used as a nuclear counterstain (blue signal), and merged images are shown. *C*, Viral load in wild-type and *Drak2*$^{-/-}$ mice. Brains were harvested at day 5 following i.c. infection. $P = 0.84 > 0.05$ for wild-type ($n = 12$) vs. *Drak2*$^{-/-}$ mice ($n = 12$).

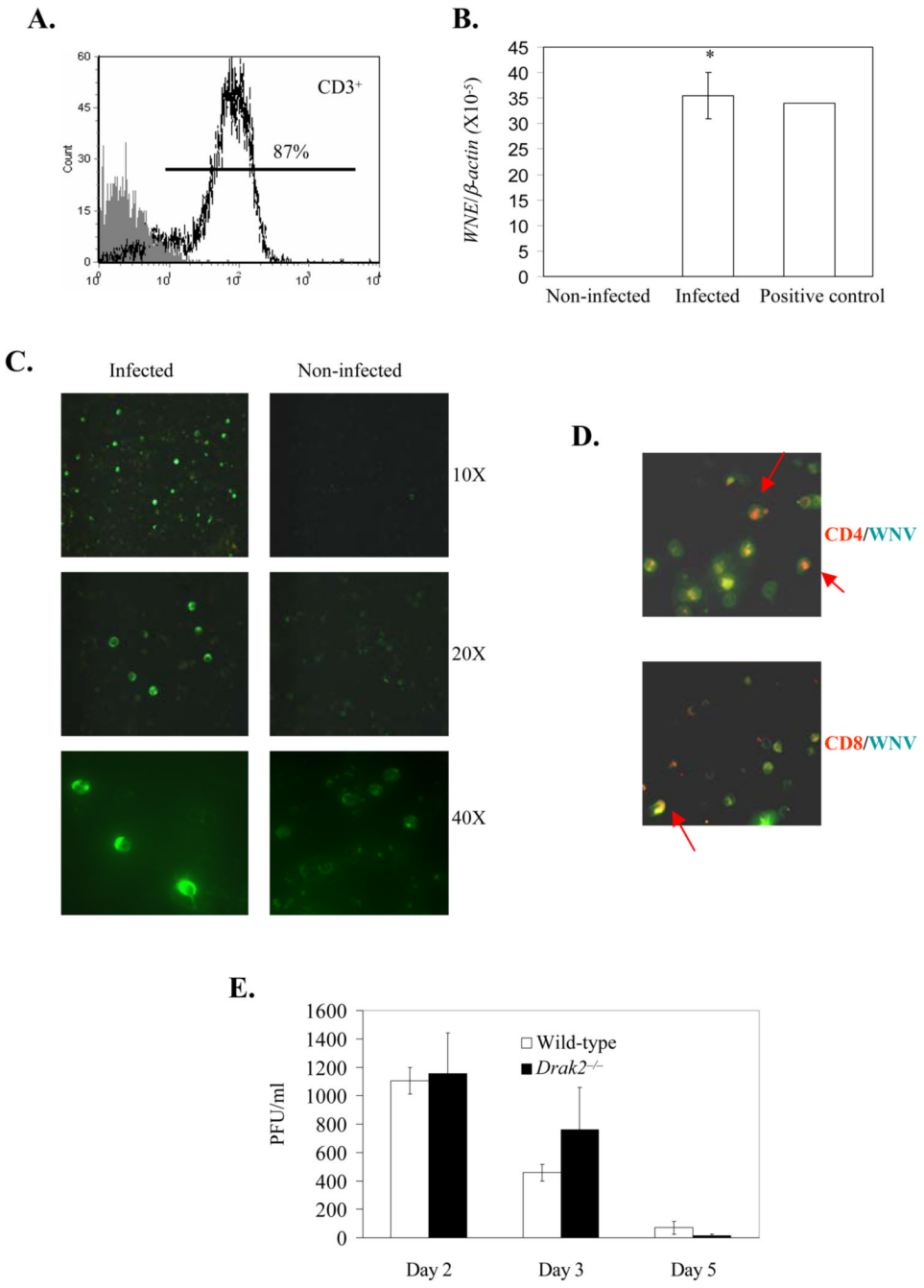

Figure 7.

T cells are permissive to WNV infection. *A*, Splenocytes from WNV infected mice were harvested at day 6 post-infection. Splenic T cells were purified with CD90 microbeads, followed by positive selection with an autoMACS Separator (Miltenyi Biotec). These T cells were stained with antibody to CD3 and analyzed by flow cytometer. Open area represents purified T cells stained with anti-CD3; gray area, unstained purified T cells. *B*, WNV infection in purified splenic T cells of infected mice as measured by Q-PCR. Negative and positive controls represent splenic T cells isolated from naïve mice and WNV infected H36.12j cells (MOI = 1, day 1 post-infection) respectively. The y-axis depicts the ratio of the amplified *WNV-E* cDNA to *β-actin* cDNA of each sample (unitless ratio ± SEM). *C*, Immunofluorescence

photomicrographs of purified splenic T cells stained for WNV antigen with various magnifications. *D*, Immunofluorescence photomicrographs of purified brain T cells isolated at day 10 post-infection. T cells were isolated by positive selection and double-stained for WNV antigen and CD4 (top panel) or CD8 (bottom panel). Arrows point to $CD4^+WNV^+$ and $CD8^+WNV^+$ populations. *E*, *In vitro* WNV infection in purified splenic T cells isolated from wild-type (n = 4) and *Drak2*$^{-/-}$ mice (n = 4) as measured by plaque assay.

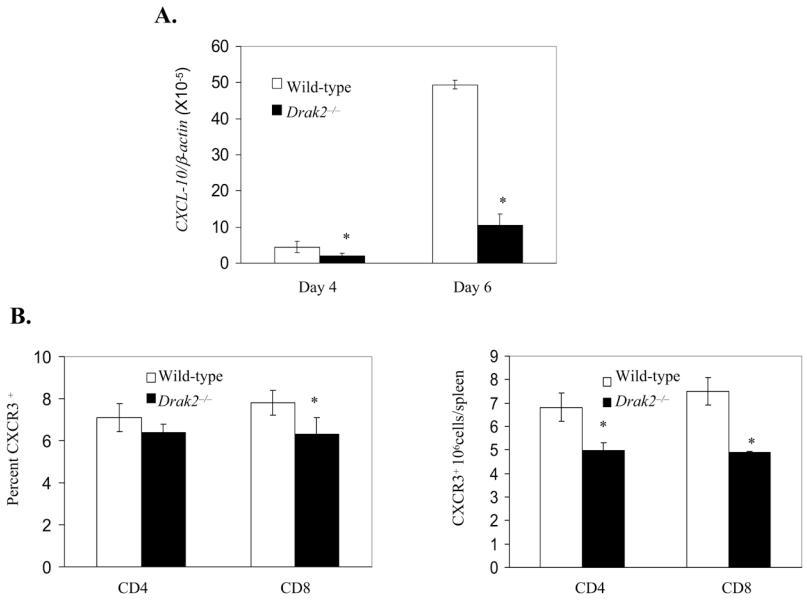

Figure 8.

Drak2 affects chemokine expression during WNV infection. *A*, CXCL10 levels in the brains of infected mice at indicated time points as measured by Q-PCR. The y-axis depicts the ratio of the amplified *CXCL10* cDNA to *β-actin* cDNA of each sample (unitless ratio ± SEM). $P < 0.05$ compared to wild-type mice. Data shown are representative of three independent experiments. $n = 4$ for each group. *B*, Peripheral CXCR3 expression was reduced on peripheral T cell surface in $Drak2^{-/-}$ mice as compared to wild-type mice. Splenocytes were stained with CD4, CXCR3 or CD8. Percent (left panel) and total number (right panel) of $CD4^+CXCR3^+$ or $CD8^+CXCR3^+$ are shown. In each experiment, three to four mice per group were analyzed. Similar experiments were repeated twice. *A value of $P < 0.05$ compared to wild-type mice.